111: Rainfall Excess Overland Flow

ROGER E SMITH[1] AND DAVID C GOODRICH[2]

[1] *Civil Engineering Department, Colorado State University, Fort Collins, CO, US*
[2] *Southwest Watershed Research Center, ARS USDA, Tucson, AZ, US*

One of the processes that can generate surface runoff is rainfall excess, which is a process controlled at the surface of the soil. This occurs when rainfall reaches the soil at a rate in excess of the soil's ability to absorb, which is called infiltrability. This dynamic property can in uniform soil be described by a rather well-developed infiltration theory. Surface water flow toward a receiving channel may in geometrically simple conditions be described by the kinematic or diffusive wave equations. The surface water is in continuous interaction with the soil's changing infiltrability. Both infiltration theory and surface flow equations are introduced here, and the interactions and complexities arising from spatial variations are discussed. These processes are incorporated in modern hydrologic response models, using numerical solutions as well as analytic solutions. The application of this theory in hydrology, however, must be informed by scale considerations and the appropriate treatment of natural complexities. Some scale limitations and some approximate methods for treating spatial soil variations are illustrated in this article, with reference to relevant literature.

INTRODUCTION

Runoff generated from storm rainfall is largely determined by local interaction of the properties of the rainfall, ground cover, land use, and soil (*see* **Chapter 117, Land Use and Land Cover Effects on Runoff Processes: Urban and Suburban Development, Volume 3** and **Chapter 118, Land Use and Land Cover Effects on Runoff Processes: Agricultural Effects, Volume 3**). While vegetation, above ground cover, and land use play a critical role in the fate of rainfall, this article focuses on the interactions between rainfall and surface soils. Here we discuss the physical dynamics of those cases where rainfall generates surface runoff at the point where it falls. *Infiltration excess* occurs when the rainfall comes at a rate higher than the rate at which the otherwise unsaturated soil can absorb water. (*Saturation excess*, discussed below, occurs when the soil is saturated or filled with water from a subsoil restriction, such as a shallow bedrock. This mechanism is not rainfall rate dependent.) The runoff or surface water flow resulting from infiltration limitation is called *infiltration excess* runoff, and the (variable) limiting soil intake rate is called the soil *infiltrability*. Infiltration excess runoff is often also referred to as *Hortonian* runoff, after Robert Horton (Horton, 1933).

The infiltration and saturation excess–generating mechanisms are not mutually exclusive on a watershed, nor even mutually exclusive at a point on a watershed. The rainfall rate may exceed the infiltrability for some storms, and for others the rain may come slowly until the surface soil layer is saturated. Climate and geography will determine which mechanism is dominant at a given location and time. Figure 1 shows a world map with climate zones indicated. The predominance of relatively short high intensity storms in most subhumid and semiarid zones means that these areas are more prone to infiltration excess runoff. Conversely, saturation excess runoff is more common in humid areas, usually characterized by greater rainfall volumes but with lower intensities. Increasingly, human activity (e.g. urbanization, compaction, etc.) results in an overall decrease of soil infiltrability resulting in globally increasing areas of infiltration excess runoff generation.

Infiltrability changes with many factors, some of which are described quantitatively here. It can also change because of changes in the soil with freezing, thawing, compaction, and tillage. An intense rain on cultivated soil

Encyclopedia of Hydrological Sciences. Edited by M G Anderson.

Figure 1 World distribution of land classes, indicating land areas subject to rainfall excess runoff. The largest grey areas correspond to semiarid and arid areas. A color version of this image is available at http://www.mrw.interscience.wiley.com/ehs

can also create a surface crust or sealed layer. While these processes have been studied and described elsewhere, they are difficult to quantify outside local conditions such as soil cover, and will be omitted from this overview.

The timescale of infiltration and surface flow processes is important, insofar as hydrologic analysis often employs lumping in space and time to approximate the behavior of hydrologic processes. Changes in soil water and changes in runoff rates occur on the order of seconds in some cases, and a timescale of a few minutes is necessary to capture the dynamics of surface runoff. By contrast, the slow movement of water in an aquifer (*see* **Chapter 112, Subsurface Stormflow, Volume 3** and **Chapter 149, Hydrodynamics of Groundwater, Volume 4**) can be characterized by timescales on the order of days or months. Thus, infiltration excess runoff is one of the more dynamic or rapidly changing fluxes in the hydrologic cycle, and as will be seen below, requires knowledge of the temporal pattern of rainfall rates to characterize it accurately.

Historical Notes

Robert Horton was one of the early proponents of the concept that higher intensity rainfall rates on soils of finer texture can exceed the intake rate of the soil and runoff thus reaches upland channels by *overland flow* on the soil surface. He also recognized the mechanism of streamflow generation by flow through the soil mantle. Recent reanalysis of Horton's data from his laboratory watershed in upstate New York indicates, not surprisingly, that the catchment included areas likely to produce a variety of runoff mechanisms, including a small marshy area (Beven, 2004).

Horton termed the limiting soil surface intake rate the "infiltration-capacity" (Horton, 1933). While he recognized that the soil intake rate decayed in value through a storm, he attributed the reduction to surface soil compaction, soil colloidal swelling, or inwashing of fines from the surface (Horton, 1939). Horton made a rather insightful analysis of the hydraulics of overland flow, but his analyses generally used constant infiltration rates. While he was aware of the prescient work of Green and Ampt (1911), he did not believe it related to catchment infiltration:

> "The question naturally arises whether the infiltration-capacity may not vary with the depth of penetration of soil-moisture into a dry soil column. Thus far, the author has not found any definite evidence of an appreciable variation in this respect. The work of Green and Ampt has a bearing on this question although their mathematical analysis of the process appears to be faulty." (Horton, 1936)

Horton further expressed his belief that the counterflow and compression of air negated the ideas of Green and Ampt. Horton's work is a good example of an early appreciation of processes at work in the field, but with a mistaken view of the relative magnitudes involved.

THE DYNAMICS OF INFILTRATION DURING STORM RAINFALL

Unsaturated Soil Hydraulic Properties

Understanding the dynamics of infiltration and runoff requires some understanding of the hydraulics of water in unsaturated soil. Soil is a *porous medium* through which water can flow even when there is air in the spaces between soil grains. Water in unsaturated soil is at a lower pressure than that of the air surrounding it, due to the *capillary pressure*, which is a property of the interface between air and water. This capillary pressure may be expressed as an equivalent (negative) head of water, with the symbol ψ, and is the same force that causes water to rise in an open capillary tube from a free source of water (*see* **Chapter 73, Soil Water Potential Measurement, Volume 2** for a more thorough discussion).

The volumetric water content of a soil, for which the symbol θ [L^3 L^{-3}] is used, varies between zero and the soil porosity, which is the relative volume of the soil not occupied by solid matter. Figure 2(a) illustrates how the soil water pressure decreases dramatically (becomes more negative) as the soil dries. This relation is often referred to as the soil water *retention* relation. Figure 2(b) illustrates by example how the soil water conductivity also falls dramatically as the soil becomes drier. *Hydraulic conductivity, K*, [$L\,T^{-1}$] is defined as the rate of flow of water in soil in response to a unit gradient of hydraulic head. The expression for this is *Darcy's Law*:

$$v = -K\frac{dH}{dz} \tag{1}$$

where v is the rate of flow in units $L\,T^{-1}$, H is hydraulic head in terms of equivalent depth of water (L), and z is the measure of distance (L). The hydraulic head, H, is made up of capillary pressure head and gravitational potential: $H = \psi + z$. Thus, in a homogeneous soil of uniform water content, and thus uniform capillary pressure head (zero capillary head gradient), water may flow downward due to gravity alone. On the other hand, unsaturated flow normal to the gravitational vector moves only in response to capillary head gradients.

In unsaturated soils, as illustrated in Figure 2(b), K is a function of capillary head, $K(\psi)$, expressed as a relative conductivity, *kr,* which is the ratio of $K(\psi)/K(0)$. $K(0)$ is called *saturated hydraulic conductivity*, K_s. K can also be treated as a function of water content, θ, through the retention relation of Figure 2(a). During rainfall infiltration, surface soil water content increases from the initial value, θ_i. For large enough rainfall rates, the surface water can reach *field saturation.* This is the water content at zero capillary head, θ_s. Further discussion of soil capillary properties can be found in article (*see* **Chapter 74, Soil Hydraulic Properties, Volume 2**), in soil physics texts, or in Smith (2002).

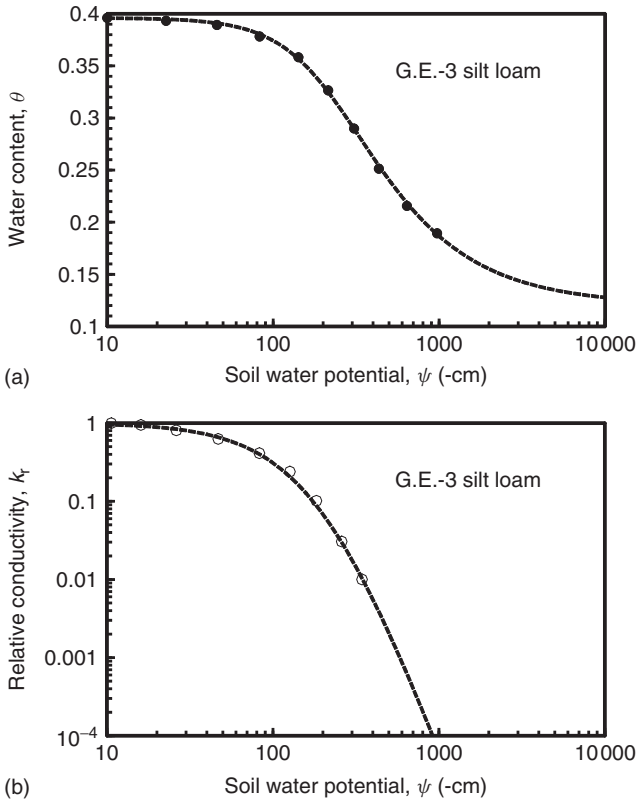

Figure 2 (a) example soil water retention curve, relating water content to soil water potential, and (b) soil relative conductivity relation for the same soil

Physical Basis of Models for Infiltration Under Rainfall

When a hypothetically unlimited supply of water initially reaches the relatively dry soil surface, the wetting at the surface creates extremely large hydraulic head gradients for flow into the soil, and the rate of influx, v, is extremely high, even though overall values of K may be low. As infiltration of rainwater continues, the hydraulic head gradient for absorption decreases, the surface value of K increases, and the rate of infiltration is dramatically reduced. When the capillary gradient at the surface ultimately approaches 0, the only head gradient is gravity, and from equation (1) it can be seen that the ultimate rate of infiltration will equal K_s.

Definitions

Hereafter, we will refer to the vertical infiltration rate at the soil surface with the symbol f. The limiting value of f, given an unlimited supply of surface water, and $\psi = 0$, is called the soil *infiltrability*, with the symbol f_c. Both vary continuously with time during rainfall as the rain intensity

and soil water conditions change. The rainfall rate, varying with time, is *r(t)*. Before a brief presentation of the origin of infiltration relations, we introduce the concept of soil water diffusivity. This concept is analogous to diffusion mathematics, where the flux of a quantity, such as heat, is a function of the gradient of that quantity. In terms of water in the soil, θ, one can use the relation illustrated in Figure 2(a) with equation (1) to obtain

$$v = D(\theta)\frac{\mathrm{d}\theta}{\mathrm{d}z} + K(\theta) \tag{2}$$

by using the definition of diffusivity, D:

$$D(\theta) \equiv K(\theta)\frac{\mathrm{d}\psi}{\mathrm{d}\theta} \tag{3}$$

Approximations for the relation $D(\theta)$ play an important role in the successful derivation of infiltrability relationships given below (Smith, 2002).

Soil Flow Dynamics and Infiltration

At the soil surface, when there is rain, the flow dynamics can be described by combining equation (2) with an expression for continuity of flow, representing the fact that the inflow rate must equal the change in soil water storage at the soil surface:

$$f = \frac{\mathrm{d}}{\mathrm{d}t}\int_0^L (\theta - \theta_\mathrm{i})\,\mathrm{d}z \tag{4}$$

where L is a depth below the advance of the wetting zone, and θ_i is assumed uniform. In this expression, we assume for relative simplicity that the initial water content is small enough for the initial downward (gravitational) flux of water to be negligible. Referring to the infiltrated water depth in the wetted soil adjacent to the surface as I, equation (4) in integral form is

$$I(t) = \int_0^t f\,\mathrm{d}t = \int_0^L (\theta - \theta_\mathrm{i})\,\mathrm{d}z \tag{5}$$

This expression in combination with Darcy's Law in the form of equation (3) yields the infiltration integral, from which at least two basic infiltration models come (see Smith, 2002 for a derivation):

$$I(t) = \int_{\theta_\mathrm{i}}^{\theta_o} \frac{(\theta - \theta_\mathrm{i})D}{v(\theta, t) - K(\theta)}\,\mathrm{d}\theta \tag{6}$$

From equation (6) and realistic assumptions about the form of the highly nonlinear functions $D(\theta)$ and $K(\theta)$ (see Parlange, *et al.*, 1982; Smith, 2002), the expressions for infiltrability are derived in terms of an important integral property of soils, called the *capillary length scale*, or capillary drive, G:

$$G = \frac{1}{K_\mathrm{s}}\int_{-\infty}^{0} K(\psi)\,\mathrm{d}\psi = \int_{-\infty}^{0} k_\mathrm{r}(\psi)\,\mathrm{d}\psi \tag{7}$$

where $\mathrm{K_s}$ is the saturated hydraulic conductivity and k_r is the relative hydraulic conductivity shown in Figure 2(b). This parameter is in effect the k_r-weighted mean value of soil capillary head. Another physically meaningful term that arises in the integration of equation (6) is the *initial water content deficit,* $(\theta_\mathrm{s} - \theta_\mathrm{i})$, hereafter referred to as $\Delta\theta_\mathrm{i}$.

Relations for infiltrability in terms of G, K_s, and the deficit, $\Delta\theta_\mathrm{i}$, include that of Green and Ampt (1911):

$$f_\mathrm{c} = \frac{K_\mathrm{s}(G\Delta\theta_\mathrm{i} + I)}{I} \tag{8}$$

and Smith and Parlange (1978):

$$f_\mathrm{c} = K_\mathrm{s}\left[1 - \exp\left(\frac{-I}{G\Delta\theta_\mathrm{i}}\right)\right]^{-1} \tag{9}$$

The infiltrability relation (8) is derived on the basis of the assumption of a $K(\psi)$ relation that approaches a step function, with K "jumping" from a negligible value to its maximum at some value of ψ (or θ) as the soil wets. This behavior is most like that of a uniform sand or silt. The relation of equation (9) is derived on the basis of the assumption that $K(\psi)$ rises exponentially as ψ increases toward 0. While this does not match the actual measured relation of most real soils, it is in most cases a better approximation than equation (8) (Parlange *et al.*, 1982).

Computational Forms for Infiltration Models

Notably, both equations (8) and (9) express infiltrability in terms of I rather than time, t. While relations between f_c, I, and time, t, can be mathematically derived, the relation of f_c to I is quite important in modeling infiltration during a storm. When a storm is sufficiently intense to create excess, the control on soil f changes from the rainfall to the infiltrability at some point. This is termed the *ponding time*. Owing to the highly nonlinear relation of $D(\theta)$, for most soil hydraulic relations there is a near equality between the infiltration relations $f_\mathrm{c}(I)$ under rainfall and that under unlimited water supply at the surface ("sudden ponding") (Smith, 2002). This allows one to use equations (8) or (9) to predict both the onset of ponding under rainfall, and the decaying function of f_c after that, when the soil exerts control through infiltrability. Because the unifying variable is I, this close approximation has been called the infiltrated depth approximation (IDA) by Smith (2002). It was earlier called the *time condensation* approximation by others (e.g. Sivapalan and Milly, 1989). The principle does not however

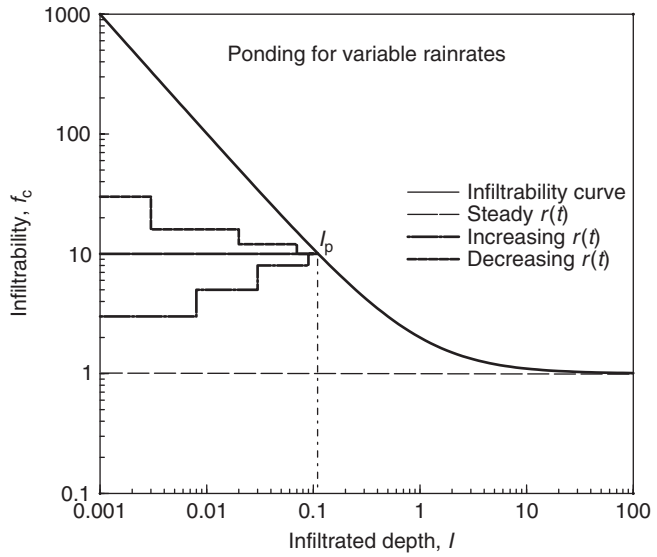

Figure 3 Relation of infiltrability to infiltrated depth, as described by equations (8) or (9), showing how ponding is predicted with this relationship. I_p is the accumulated infiltration depth at ponding

actually relate to the condensation of time. It assumes that the time at which the surface boundary condition changes from rainfall to soil control occurs when the relation between r and I_a matches that for $f_c(I_a)$, where I_a is the accumulated infiltration due to rainfall. This is termed the time of ponding, and subsequent variables with subscript p (such as I_p) refer to the value of the variable at that time. Figure 3 illustrates the fact that in the *f(I)* relation, ponding at I_p may be approached by any number of patterns of rainfall.

Nondimensional Forms

Different soils have a wide range of values of the hydraulic parameters G, K_s, and the initial soil deficit $\Delta\theta_i$ varies between storms. The infiltration equations may be unified and simplified by producing dimensionless forms, scaling I by the value of $G\Delta\theta_i$, and scaling f_c on K_s:

$$f_{c^*} = \frac{f_c}{K_s} \qquad I_* = \frac{I}{G\Delta\theta_i} \tag{10}$$

These dimensionless forms were used in Figure 3. Equation (8), using these variables, is thereby simplified to

$$f_{c^*} = \frac{I_* + 1}{I_*} \tag{11}$$

A dimensionless time may similarly be found:

$$t_* = \frac{t}{G\Delta\theta K_s^{-1}} \tag{12}$$

and rainfall rate may be scaled as for infiltrability: $r_* = r/K_s$. Relations between time and either I_* or f_{c^*} are obtained by substituting the relation $f_* = \mathrm{d}I_*/\mathrm{d}t_*$ into equations (8) or (9). The resulting expressions are implicit in time, but explicit expressions have been presented by Smith (2002), Paige *et al.* (2002), and Li *et al.* (1976), one of which will be presented here.

Infiltrability as a Function of Time

Time-explicit expressions are useful after ponding has been found using the IDA. The simplest approximate expression for post-ponding $f_{c^*}(t_*)$ can be given as (Smith, 2002):

$$f_{c^*} = (1 - \beta) + \sqrt{\beta^2 + \frac{1}{2t'_*}} \tag{13}$$

where β is a weighting parameter. This expression describes a relation intermediate between that of equations (8) and (9) for values of β between 0.5 and 1. Figure 4 illustrates the time-explicit equation (13) and time-f_c relations for both equations (8) and (9). The physics of infiltration requires that at small times the functions must be asymptotic to the line $f_{c^*} = (t_*)^{-1/2}$, and at large times asymptotic to $f_{c^*} = 1$. The variable t' is used to indicate that the time position of this curve must be adjusted to describe f_c after ponding time, t_p, (or ponding depth I_p) so that $f_{c^*} = r_{p^*}$ at $t'_* = t_{p*}$, where r_p is the rainfall rate at which ponding occurs. Using infiltrability expression, equation (9) for example, and solving for $I = I_p$ expressed as an integral of the rainfall rate pattern, the ponding time is found using the

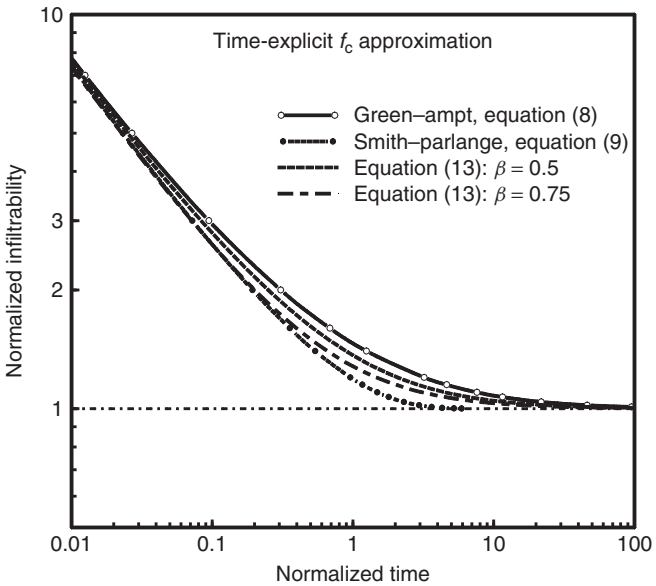

Figure 4 Illustration of the ability of the time-explicit $f_c(t)$ equation (13) to match the behavior of equations (8) and (9) when put in $t(f_c)$ form

IDA method:

$$I_p = \int_0^{t_p} r(t)\,\mathrm{d}t = G\Delta\theta_i \ln\left(\frac{r_*}{r_* - 1}\right) \qquad (14)$$

Clearly, the ponding time $t_p(r)$ can be determined directly for a rainfall of constant rate, for which $I = rt$. After ponding occurs, the infiltrability expression equations (8), (9), or (13) will estimate rainfall excess during the period of time when surface available water, including the rainfall and ponded water, equals or exceeds the infiltrability. This leads to the consideration of the dynamic interaction of infiltration and surface water flow, discussed below.

Irregular Rainfall and Recovery of Infiltrability During Rainfall Hiatus

The above methodology is robust for an unlimited variation in the pattern of rainfall, with the caveat that rainfall must stay greater than K_s, that is, $r_* > 1$. For the more general case, there needs to be an accounting for redistribution of water during breaks in rainfall (periods when $r = 0$), or any time infiltrability exceeds the rainfall. Local conditions can easily be simulated, given the soil hydraulic properties, by solution of the nonlinear convection diffusion equation (Richards' equation; *see* **Chapter 150, Unsaturated Zone Flow Processes, Volume 4** and **Chapter 66, Soil Water Flow at Different Spatial Scales, Volume 2**), but this is not practical for most hydrological catchment models. Some early methods for treating breaks in rainfall patterns simply maintained a value of I through the hiatus (e.g. Mls, 1980). Corradini *et al.* (1997) and Smith *et al.* (1999) have proposed and demonstrated a method of intermediate complexity requiring minimum parameterization of the soil hydraulic properties, which simulates robustly the changes in infiltrability and soil water deficit $\Delta\theta_i$ for periods when rainfall rates fall to any value less than K_s. This method treats the wetting pulse in the soil as a distortable curve with conserved similarity and net volume of water, with Green–Ampt type assumptions on its distortion (changes in depth and surface water content) under low (or negative) surface flux values. The reader is directed to the above references, or Smith (2002), for details.

Surface Water and Infiltration Interdependence

Early methods of treating infiltration excess involved subtracting an infiltration pattern (often assumed constant) from the rainfall pattern and then routing the remainder ("rainfall excess") across the catchment toward a receiving stream (Crawford and Linsley, 1966; HEC-1, 1990). Not only does this ignore the interaction of rainrate and ponding time described above, which was generally unknown, but it also ignores the ability of the soil to continue to infiltrate whatever surface water exists after rainfall has fallen below the infiltrability. The result was an inability to estimate ponding time and an overestimation of the recession flow after runoff production had ceased. Also important in the interactions of surface water and infiltration is the microtopography of the surface and the spatial variability of infiltrability. Microtopography can confine the flowing water to some fraction of the total area, and thus limit the opportunity for infiltration losses during recessions. Significant spatial variability of infiltrability is known to vary on length scales as small as decimeters. These topics will be explored in more detail below.

RUNOFF DYNAMICS

The flow of the rainwater not infiltrated by the soil surface (rainfall excess) is at the small (mm) scale, a complex phenomenon with exact flow directions, unit discharges (discharge per unit flow width), and depths varying widely across the surface (Abrahams and Parsons, 1994; Fiedler and Ramirez, 2000). Runoff is, however, treated at a larger (m) scale as a free-surface hydraulic process. The physical description involves some reasonable assumptions that yield a useful and relatively accurate mathematical description of the runoff from most natural surfaces. Figure 5 illustrates diagrammatically the variables involved in the flow of water along a simplified hillslope.

The Surface Water Flow Equations

The primary assumption is that flow is downslope and locally can be approximated as one-dimensional. At larger scales, it is clearly two-dimensional as the land surface converges and diverges downslope, but even this may be treated as stepwise one-dimensional. The flow is incompressible, and the overall velocity is sufficiently low that the energy is largely in the form of momentum. Thus, the equations used are those that conserve momentum and mass. These equations were first written by de Saint Venant (1871), and are commonly referred to as the Saint Venant equations. The two equations include the conservation of momentum

$$\frac{\partial u}{\partial t} + u\frac{\partial u}{\partial x} + g\frac{\partial h}{\partial x} = g(S_o - S_f) - \frac{u}{A}(r - a_f f) \qquad (15)$$

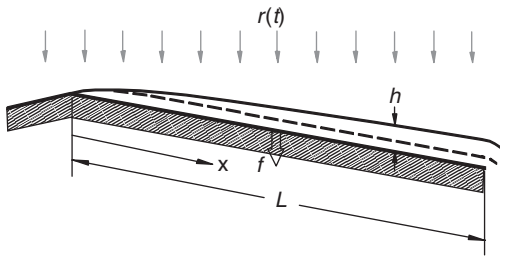

Figure 5 Definition diagram for kinematic approximation for runoff water dynamics

and the conservation of mass

$$\frac{\partial A}{\partial t} + \frac{\partial Q}{\partial x} = (r - a_f f)w \tag{16}$$

where

A is cross-sectional area of flow [L^2]
a_f is fraction of surface covered by infiltrating water
Q is discharge per unit width [$L^2\ T^{-1}$]
x is distance from upstream border [L]
t is time
u is flow velocity [$L\ T^{-1}$]
h is mean depth of flow [L]
g is gravitational acceleration [$L\ T^{-2}$]
S_o is mean bed slope
S_f is friction slope
w is width of flow [L].

The first terms in equation (15) represent changes in momentum and potential energy, and the last term on the right represents the change in momentum due to lateral inflows. The infiltrating area fraction a_f is 1.0 when $r > f_c$, and is reduced on irregular surfaces during flow recession when infiltration comes from surface water. The friction slope represents the shear friction along the flow perimeter, and is exemplified by the Chezy or Manning equation:

$$q = \alpha h^m = \frac{\sqrt{S_f}}{n} h^{5/3} \tag{17}$$

where q is unit discharge [$L^2\ T^{-1}$], α and m are the generalized friction relation parameters, and n is the Manning friction factor. Equation (17) represents experimental results from channels, in which hydraulic radius R replaces h, but the power law relation also reflects considerable experimental data from catchment experiments (e.g. Wu *et al.*, 1978; Abrahams and Parsons, 1994; Emmett, 1970). The form of the friction slope relation is also applicable to the Chezy friction law relationship ($m = 3/2$) (Eagleson, 1970). Note that h represents the mean depth or area per unit width. The relationship described by equation (17) simply states that the unit discharge is a function of a modeled average depth (or storage) in the abstract sheet flow representation of overland flow depicted in Figure 5. It does not imply that overland sheet flow must occur on a hillslope to represent the flow dynamics described in equations (15) through (17). While overland sheet flow has been observed in field settings (e.g. Emmett, 1970), it is not typical as surface water flows usually converge to rivulets in a relatively short distance due to natural microtopography (Dunne, *et al.*, 1991) (also *see* **Chapter 11, Upscaling and Downscaling – Dynamic Models, Volume 1**). The appropriateness of the discharge-storage relationship implied by equation (17) has been evaluated by several including Wu *et al.* (1978), as well as by microscale numerical simulation with a two-dimensional form of equations (15) and (16) (Fiedler and Ramirez, 2000).

Simplified Forms

The Saint Venant equations are generally applicable to channel and streamflow, but further simplifications are appropriate for overland flow. Because flow is shallow, it can be reasonably assumed that very little energy is contained in the form of inertia, and an order of magnitude analysis demonstrates that the addition of rainfall excess adds negligible net momentum to the flow. With these approximations, equation (15) can be reduced to

$$\frac{\partial h}{\partial x} = S_o - S_f \tag{18}$$

Equations (17) and (18) constitute the *diffusive wave equations* (Morris and Woolhiser, 1980), which are appropriate for certain flow conditions characterized by shallow slopes. A criterion for applicability is given by Morris and Woolhiser (1980).

For larger values of surface slope S_o, the value of dh/dx becomes negligible compared with S_o, and equation (18) reduces to $S_f = S_o$. In this case, the *kinematic wave equations* are appropriate. The flow-depth relationship in this case is a description of the relation of mean effective depth and mean effective discharge, equation (17). This relation plus the continuity of mass equation (16) constitute the kinematic wave equations. Equation (16) with equation (18) may be written in terms of h for unit width of overland flow, rather than area A:

$$\frac{\partial h}{\partial t} + m\alpha h^{m-1} \frac{\partial h}{\partial x} = r - a_f f \tag{19}$$

Woolhiser and Liggett (1967) developed a kinematic wave number, $k = S_o L / h_o F^2$, to measure the ability of equation (19) to represent well the Saint Venant equations. L is plane length, h_o is normal depth for a given flow q, and F is Froude number. Larger values of k indicate that the kinematic wave equations are better approximations. This analysis was further extended by Morris and Woolhiser (1980) to consider a larger range of Froude numbers.

Solving the Kinematic Wave Equations

Equation (19) may be solved under certain assumptions by use of the method of characteristics. This is a mathematical approach to solve sets of partial differential equations by transformation into sets of ordinary differential equations (Lighthill and Whitham, 1955; Wooding, 1965). This article is not an appropriate place to present the details of this method, but it is instructive to look briefly at the solution, as it describes the behavior of a surface water runoff hydrograph.

Characteristics are traces in the solution domain (in this case the x, t plane) along which a partial differential equation is reduced to an ordinary differential equation. The characteristic equations corresponding to equation (19) are as follows:

$$\frac{dx}{dt} = \alpha m \sqrt{S_o} h^{m-1} \tag{20}$$

$$\frac{dh}{dt} = r - a_f f \tag{21}$$

Equation (20) describes the *celerity* or characteristic velocity of the flow. In the characteristic method, equation (21) is valid along the line described in the (x, t) plane by equation (20). In turn, the change in h described by equation (21) changes the slope of the x, t characteristic.

Figure 6 illustrates some of the essential features of the characteristics as runoff begins along a slope. This is a very simplified schematic, but at some time after the start of rainfall, runoff begins. The upstream characteristic starts at $x = 0, t = 0$, and moves at an increasing rate downslope. To the right of this characteristic, the flow is unsteady and uniform. To the left, flow is steady and nonuniform. When the upstream characteristic reaches the lower bound, outflow becomes steady, and this is termed the *time to equilibrium*. In this example, and for many rainfalls and short runoff surfaces, this condition is not reached. After the end of rainfall, the characteristics exhibit decelerating celerities as $h(x)$ is reduced by infiltration, and at some time the characteristic velocity and h fall to zero. The locus of drying is shown on the schematic. Between the end of rainfall and the end of runoff, the hydrograph is in *recession*. For impervious surfaces where $f = 0$, the recession is extended considerably, and the recession characteristics are straight lines of differing slopes that depend on $h(x)$ at the time rainfall excess ends.

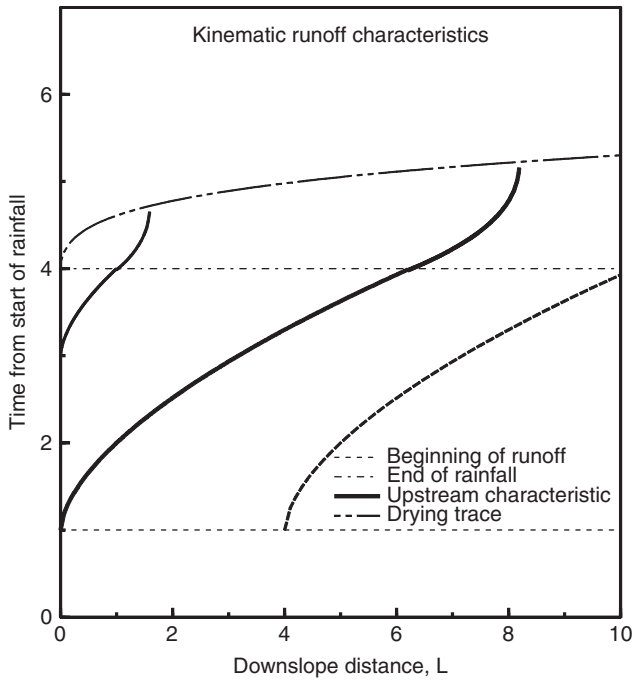

Figure 6 Solution of the kinematic wave equations in the (x,t) plane, for runoff assumed to start at $t = 1$ and end at $t = 4$. The dotted line in Figure 5 illustrates the water depth profile for a time (approximately = 2) when most of the surface is characterized by uniform unsteady flow

Computer models of runoff generally approach the solution of equation (19) with numerical methods, which can treat the time variation of f directly if not analytically. Several early numerical methods have been discussed by Brakensiek *et al.* (1966), and the robust *weighted implicit method* is described by Smith *et al.* (1995b). The characteristic solution is used in this model to estimate the arrival of the upstream characteristic at the first finite difference space node to prevent small solution oscillations. A full discussion of the merits and drawbacks of the various numerical solution techniques is beyond the scope of this article.

SURFACE AND SOIL WATER INTERACTION

It is through the right-hand term in equation (19) that the equations of surface water flow and the equation describing surface water infiltration are linked. From the point of view of the surface water calculations at any point, the input to surface flow is always $r - f$, and becomes negative (a loss) when the rainfall rate, r, falls below f_c, as long as there is free water on the surface. From the point of view of the infiltration calculations after runoff begins, the reduction of rainfall rate below f_c is not noticed, and infiltration rate continues at capacity f_c, as long as this rate can be supplied by surface water plus rainfall rate.

The solution characteristics during recession are also shown schematically in Figure 6. The case of a "flat" infiltrating surface and an impervious surface are two extremes in the behavior of the flow recession. Intermediate to these two is the case of a surface with microtopographic features, either irregular – such as grassed hummocks, or regular, such as furrowed paddocks. In this case, the area available for infiltration during recession flow is a function of the mean depth of surface water. The area is clearly zero at $h = 0$, and at some rather large depth, h_c, the entire area may be covered with water. For $0 < h < h_c$, a fraction of the area will be covered and the loss of water to infiltration during recession will be limited accordingly.

Another case where microtopography plays an important role in surface water interactions is the case of *run-on*. This term refers to situations where water is generated by rainfall excess at a location upslope or upstream of an area with a higher infiltration capacity. Surface microtopography and resulting flow convergence can limit the opportunity for infiltration of the run-on water as the effective wetted

perimeter is reduced. This in turn can affect the extent to which run-on will advance across the irregular surface. Woolhiser *et al.* (1996) studied, for example, the case of run-on caused by a spatial trend in infiltration due to variation in K_s, and showed that significant effects on hydrographs are possible. Small-scale random spatial variations are a somewhat different case.

Spatial Variability and its Effects on Runoff Processes

Like most natural processes, infiltration excess and its associated runoff are affected by the variability of nature. Some natural processes lend themselves to treatment in bulk, with processes characterized by parameters that represent the sum effect of many smaller scale variations. Runoff tends, however, to be a nonlinear process in many locations, and it is often affected by natural spatial variations at scales an order of magnitude less than the scale of interest (*see* **Chapter 3, Hydrologic Concepts of Variability and Scale, Volume 1**).

In applying the kinematic flow equations, microtopography can be abstracted to a simple microchannel geometry (Woolhiser, *et al.*, 1996; Smith *et al.*, 1995a). This can represent the ensemble result of extensive measurements of variations in relief across the flow direction, such that a composite geometry may represent the relative surface coverage between mean depths of 0 and some maximum.

Small-scale variations in surface conditions or soil conditions within a catchment can make it difficult to represent the catchment runoff processes by the mathematics described above. The infiltration parameter K_s is a very important one in estimating infiltration and runoff dynamics for Hortonian runoff, and it has been found consistently to exhibit random variation at small scales (cm to m) (Nielsen *et al.*, 1973). Several methods have been reported to deal with the effect of this variation on the runoff for small catchments (Smith and Hebbert, 1979; Sivapalan and Wood, 1986; Sharma *et al.*, 1980; Smith and Goodrich, 2000). In general, the difference between infiltration at a point and the behavior of an ensemble of points is illustrated in Figure 7. This graph uses scaled values as described by equations (10) and (11). The local value of K_s is assumed, on the basis of experimental evidence, to vary randomly with a lognormal distribution. The effect of random variation is to blur the existence of a single time of ponding, as shown, and further to alter the value of the large-time asymptotic value of f_c. The effect of variability on K_s is largely confined to smaller values of rainfall rate; for r_* values of 10 or more, where $r_* \geq$ the highest infiltration capacity, it is negligible. On the basis of the value of the coefficient of variation of K_s [CV(K_s)], Smith and Goodrich (2000) developed an ensemble infiltration model that uses the same parameters as equations (8) or (9), but includes the effect of CV(K_s) and rainfall rate.

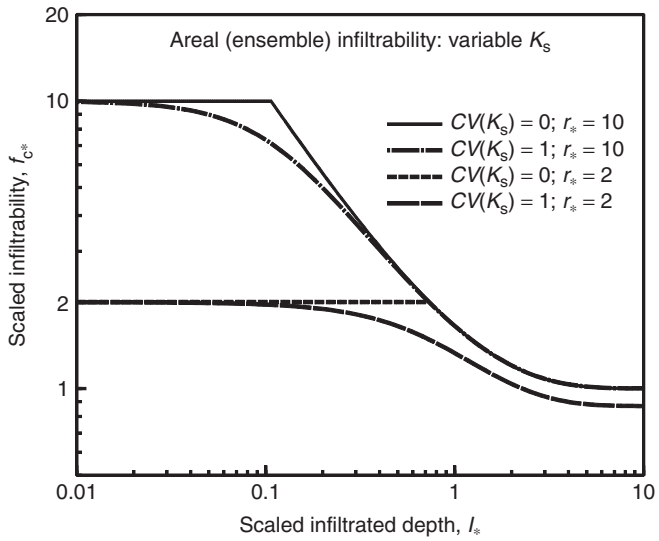

Figure 7 Examples of infiltration patterns for areas characterized by small-scale variability of K_s. Two rainfall rates are shown, and the interaction of variability and rainrate is illustrated

The effect of parameter variations in looking at larger-scale hydrology is an important problem related to *upscaling* in hydrology – simulating or predicting the performance of an ensemble of catchments that make up a larger catchment. Models of hydrology useful at one scale may not be successful at the scale an order or more larger. While the functional representation of small-scale K_s variations improves the prediction of runoff, especially for storms where the runoff is a small fraction of the rainfall, the interactions of variability during runoff are more complicated than the ensemble effect, due to run-on along the flow path. Another method to treat this, at least in a research-level model, distributes finite incremental variations in values of K_s randomly along the flow in a one-dimensional simulation, or divides the catchment into parallel strips of flow, each strip representing a portion of the random distribution expected in the value of K_s (Woolhiser and Goodrich, 1988).

Other characteristics of a catchment may also exhibit significant spatial variability. The effects of variation in slope and surface hydraulic roughness can be modeled at appropriate scales by treating the flow path as a cascade of smaller elements (Smith *et al.*, 1995b; Goodrich *et al.*, 2002; see also **www.tucson.ars.ag.gov/kineros**). This becomes impractical at very small or large scales; however, surface runoff becomes channelized into rills and microchannels before the scale becomes too large to consider such variations.

The scale of variation of runoff intensity is generally larger than that of K_s, but its variation is equally as important for treating infiltration excess on a catchment. Spatial

variability of rainfall and its effects on runoff generation on catchments scales of $1-100\,km^2$ and greater have been relatively widely studied (Balmer *et al.*, 1984; Iwasa and Sueishi, 1990; Niemczynowicz and Sevruk, 1991; Houser *et al.*, 2000; Syed *et al.*, 2002), with those at smaller areal scales typically geared toward urban storm runoff estimation (Berne *et al.*, 2004). Even in an urban setting, the normal scale of rainfall measurements, including those derived from radar, are often considerably larger than rainfall variations that are important for runoff generation. This is particularly true where small intense runoff-producing storm cells dominate runoff production. The USDA-ARS Walnut Gulch Experimental Watershed (WGEW) in southeast Arizona is such an area. In this experimental watershed, Reich and Osborn (1982) concluded that for 5-min maximum storm depths recorded at rain gauges greater then 5 km apart were statistically independent. At a smaller scale within the WGEW (~5 hectare catchment area), Goodrich *et al.* (1995) found rainfall gradients ranging from 0.28 to 2.48 mm/100 m with an average of 1.2 mm/100 m. These gradients represent a 4 to 14% variation of the mean rainfall depth over a 100-m distance but a much larger percentage in terms of total depth of runoff over the catchment due to the relatively low runoff to rainfall ratios that are common in arid and semiarid regions. In a follow-on study, Faurès *et al.* (1995) found that if distributed catchment modeling is to be conducted at the 5-hectare scale, knowledge of the spatial rainfall variability on the same or smaller scale is required. A single raingage with the standard uniform rainfall assumption can lead to large uncertainties in runoff estimation.

Scale Issues and Models of Runoff

Finally, it is important to consider the timescales of the processes of surface runoff. Surface water flows on natural topography do not travel far before converging in some manner into concentrated flow channels. Distributed surface flows prior to some kind of channelization rarely exceed 100 m in length, except in special cases of low-sloped tilled catchments (Dunne *et al.*, 1991; Abrahams and Parsons, 1994). This limitation in spatial scale also imposes a limitation in timescale. The timescale of variations and the rate of flow across the surface means that rainfall rate variations on the order of less than a minute can be important parts of the dynamics of runoff. Surface runoff cannot therefore be treated scientifically with information on rainfall that consists only of the daily depth of rain. For this lumped data approximation, the prediction of runoff will contain enormous uncertainty.

Models of Hortonian runoff generally employ the solution of the kinematic or diffusive wave equations by numerical methods. The wide variety of numerical solution is too numerous to be described here. Readers are referred to Singh (1995) for a good overview of numerical solution techniques. Again, there are practical limits for the numerical subdivision of the flow path, and these impose corresponding limits on the timescales. Moreover, the values of h that are involved in the solution are on the order of a few millimeters, and the solution of equation (19) over values of Δx that are tens or even hundreds of meters or longer are physically realistic treatments of shallow flow dynamics, but are rather simply nonlinear storage models. While some models have employed runoff elements at this scale, a valid numerical model of surface runoff should be confined to the length of flow expected before rills, channels, and other cascading concentrated flow paths begin to dominate the runoff hydraulics. If concentrated flows and rills do not dominate the hydraulics, changes in slope and convergence of flow can both be modeled by the use of cascading one-dimensional surfaces with varying slopes and widths (Woolhiser *et al.*, 1990; Smith *et al.*, 1995b).

SUMMARY

We have briefly shown how the theory of soil and surface water hydraulics has led to a model of surface water generation from rainfall for catchments on the scale of hectares. However, this should not tempt us to believe that a scientific knowledge of rainfall excess can easily be applied to hydrologic problems in general. The models are at best quasi-scientific insofar as nature's ubiquitous heterogeneities do not allow the hydrologist to make direct measurements at any point of many of the important parameters (e.g. surface roughness), or even determine a real effective average of parameters by any remotely sensed data. The theoretical basis of the processes described above does allow some confidence in the robustness of estimated parameters insofar as they are applicable to a wide range of rainfall conditions, but direct measurement of key properties, such as effective catchment values for K_s, remains a difficult undertaking.

Remotely derived topographic data using LIDAR is of sufficient accuracy and resolution that it can be used to aid in estimation of some of the geometric parameters (slopes and slope lengths, etc.) required for excess rainfall-runoff modeling (Carter *et al.*, 2001). Multispectral remotely sensed data has been widely used to estimate land use and ground cover, and if sufficient temporal resolution exists, the variation of ground cover conditions can affect hydraulic roughness and influence infiltration parameters. Land use and land cover data, combined with textural-based estimates of soil hydraulic properties can be used to provide crude initial estimates of needed parameters (Miller *et al.*, 2002; and see **www.tucson.ars.ag.gov/agwa**). However, these estimates are often based on simple look-up table relationships from incomplete field data relating soils and cover to surface and soil hydraulic parameters. This leaves hydrologic science with challenges for field data

collection and realistic characterization of the variability of important parameters for use in the mathematical models of rainfall excess runoff described herein.

REFERENCES

Abrahams A.D. and Parsons A.J. (1994) Hydraulics of interrill overland flow on stone-covered desert surfaces. *Catena*, **23**, 111–140.

Balmer P., Malmqvist P.A. and Sjoberg A. (Eds.) (1984) *Proceedings of the Third International Conference on Urban Storm Drainage*, Vol. 4, Published by Chalmers University of Technology: Goteborg, June 4–8, 1984.

Berne A., Delrieu G., Creutin J.-D. and Obled C. (2004) Temporal and spatial resolution of rainfall measurements required for urban hydrology. *Journal of Hydrology*, **299**(3–4), 166–179.

Beven K.J. (2004) Surface runoff at the Horton Hydrologic Laboratory. *Journal of Hydrology*, **293**, 219–234.

Brakensiek D.L., Heath A.L. and Comer G.H. (1966) *Numerical Techniques for Small Watershed Flood Routing*, U.S. Department of Agriculture, ARS 41–113.

Carter W., Shrestha R., Tuell G., Bloomquist D. and Sartori M. (2001) Airborne laser swath mapping shines new light on earth's topography. *EOS, Transactions-American Geophysical Union*, **82**(46), 549, 550, 555.

Corradini C., Melone F. and Smith R.E. (1997) A model for infiltration during complex rainfall patterns. *Journal of Hydrology*, **192**, 104–124.

Crawford N.H. and Linsley R.K. (1966) *Digital Simulation in Hydrology*, Stanford Watershed Model IV, Stanford University Technical Report No. 39, Palo Alto.

de Saint Venant B. (1871) Théorie du movement non-permanent des eaux avec application aux crues des revierés *et al.*'introduction des marées dans leur lit. *Academie Des Sciences [Paris] Comptes*, **73**, 148–154, 237–240.

Dunne T., Zhang W. and Aubry B.F. (1991) Effects of rainfall, vegetation, and microtopography on infiltration and runoff. *Water Resources Research*, **27**(3), 2271–2285.

Eagleson P.S. (1970) *Dynamic Hydrology*, McGraw Hill: New York, pp. 325–367.

Emmett W.W. (1970) *The Hydraulics of Overland Flow*, USGS Profession Paper 662-A, US Government Printing Office: Washington.

Faurès J.M., Goodrich D.C., Woolhiser D.A. and Sorooshian S. (1995) Impact of small-scale spatial rainfall variability on runoff simulation. *Journal of Hydrology*, **173**, 309–326.

Fiedler F.R. and Ramirez J.A. (2000) A numerical method for simulating discontinuous shallow flow over an infiltrating surface. *International Journal for Numerical Methods*, **32**, 219–240.

Goodrich D.C., Faurès J.M., Woolhiser D.A., Lane L.J. and Sorooshian S. (1995) Measurement and analysis of small-scale convective storm rainfall variability. *Journal of Hydrology*, **173**, 283–308.

Goodrich D.C., Unkrich C.L., Smith R.E. and Woolhiser D.A. (2002) KINEROS2 – a distributed kinematic runoff and erosion model. *Proceedings of the Second Federal Interagency Hydrologic Modeling Conference*, Las Vegas, p. 12, July 28 – August 1, 2002.

Green W.A. and Ampt G.A. (1911) Studies on soil physics: 1. The flow of air and water through soils. *Journal of Agricultural Science*, **4**, 1–24.

Horton R.A. (1933) The role of infiltration in the hydrologic cycle. *Transactions-American Geophysical Union*, **14**, 446–460.

Horton R.A. (1936) Hydrologic interrelations of water and soils. *Soil Science Society of America Proceedings*, **1**, 401–429.

Horton R.A. (1939) Analysis of runoff-plot experiments with varying infiltration-capacity. *Transactions of the American Geophysical Union*, **20**(Part IV), 693–711.

Houser P.R., Goodrich D.C. and Syed K.H. (2000) Runoff, precipitation, and soil moisture at Walnut Gulch. In *Spatial Patterns in Hydrological Processes: Observations and Modeling*, Chap. 6, Grayson R. and Blosch G. (Eds.), Cambridge University Press: pp. 125–157.

Hydrologic Engineering Center (1990) *HEC-1, Flood Hydrograph Package, Users Manual*, USACE HEC Publication CPD-1A, p. 433.

Iwasa Y. and Sueishi T. (1990) *Proceedings of the Fifth International Conference on Urban Storm Drainage*, Published by University of Osaka: Osaka, July 23–27.

Li R.M., Stevens M.A. and Simons D.B. (1976) Solutions to the Green-Ampt infiltration equation. *Journal of Irrigation and Drainage, ASCE*, **102**(2), 239–248.

Lighthill F.R.S. and Whitham G.B. (1955) On kinematic waves, 1. Flood movement in long rivers. *Proceedings of the Royal Society of London, Series A*, **239**, 281–316.

Miller S.N., Semmens D.J., Miller R.C., Hernandez M., Goodrich D.C., Miller W.P., Kepner W.G. and Ebert D. (2002) GIS-based hydrologic modeling: the automated geospatial watershed assessment tool. *Proceeding of the Second Federal Interagency Hydrologic Modeling Conference*, Las Vegas, p. 12, July 28 – August 1, 2002.

Mls J. (1980) Effective rainfall estimation. *Journal of Hydrology*, **45**, 305–311.

Morris E.M. and Woolhiser D.A. (1980) Unsteady one-dimensional flow over a plane: partial equilibrium and recession hydrographs. *Water Resources Research*, **16**(2), 355–360.

Nielsen D.R., Biggar J.W. and Erh K.T. (1973) Spatial variability of field measured soil water properties. *Hilgardia*, **42**, 215–260.

Niemczynowicz J. and Sevruk B. (1991) Urban rainfall and meteorology. *Atmospheric Research*, **27**(1–3), 215.

Paige G.B., Stone J.J., Guertin D.P. and Lane L.J. (2002) A strip model approach to parameterize a coupled Green-Ampt kinematic wave model. *Journal of American Water Resources Association*, **38**(5), 1363–1377.

Parlange J.-Y., Lisle I., Braddock R.D. and Smith R.E. (1982) The three-parameter infiltration equation. *Soil Science*, **133**(6), 337–341.

Reich B.M. and Osborn H.B. (1982) *Improving Point Rainfall Prediction with Experimental Data, International Statistical Analysis of Rainfall and Runoff. International Symposium on Rainfall/Runoff*, Mississippi State University, Water Resources Publication: Littleton, pp. 41–54.

Sharma M.L., Gander G.A. and Hunt C.G. (1980) Spatial variability of infiltration in a watershed. *Journal of Hydrology*, **45**, 101–122.

Singh V.P. (Ed.) (1995) *Computer Models of Watershed Hydrology*, Water Resources Publications: Highlands Ranch.

Sivapalan M. and Milly P.C.D. (1989) On the relationship between the time condensation approximation and the flux-concentration relation. *Journal of Hydrology*, **105**, 357–367.

Sivapalan M. and Wood E.F. (1986) Spatial heterogeneity and scale in the infiltration response of catchments. In *Scale Problems in Hydrology*, Chap. 5, Gupta V.K., Rodriguez-Iturbe I. and Wood E.F. (Eds.), Reidel: Hingham, pp. 81–106.

Smith R.E. (2002) *Infiltration Theory for Hydrologic Applications*, *Water Resources Monograph 15* , American Geophysical Union: Washington.

Smith R.E., Corradini C. and Melone F. (1999) A conceptual model for infiltration and redistribution in crusted soils. *Water Resources Research*, **35**(5), 1385–1393.

Smith R.E. and Goodrich D.C. (2000) Model for rainfall excess patterns on randomly heterogeneous areas. *Journal of Hydrologic Engineering, ASCE*, **5**(4), 355–362.

Smith R.E., Goodrich D.C. and Quinton J.N. (1995a) Dynamic, distributed simulation of watershed erosion: the KINEROS2 and EUROSEM models. *Journal of Soil and Water Conservation*, **50**(5), 517–520.

Smith R.E., Goodrich D.C., Woolhiser D.A. and Unkrich C.L. (1995b) KINEROS – a kinematic runoff and erosion model. In *Computer Models of Watershed Hydrology*, Chap. 20, Singh V.J. (Ed.), Water Resources Publication: Highlands Ranch, pp. 697–732.

Smith R.E. and Hebbert R.H.B. (1979) A Monte-Carlo analysis of the hydrologic effects of spatial variability of infiltration. *Water Resources Research*, **15**(2), 419–429.

Smith R.E. and Parlange J.-Y. (1978) A parameter-efficient hydrologic infiltration model. *Water Resources Research*, **14**(3), 533–538.

Syed K., Goodrich D.C., Myers D. and Sorooshian S. (2002) Spatial characteristics of thunderstorm rainfall fields and their relation to runoff. *Journal of Hydrology*, **271**(1–4), 1–21.

Wooding R.A. (1965) A hydraulic model for the catchment-stream problem. I. Kinematic wave theory. *Journal of Hydrology*, **3**, 254–267.

Woolhiser D.A. and Goodrich D.C. (1988) Effect of storm rainfall intensity patterns on surface runoff. *Journal of Hydrology*, **102**, 335–354.

Woolhiser D.A. and Liggett J.A. (1967) Unsteady one-dimensional flow over a plane – The rising hydrograph. *Water Resources Research*, **3**, 753–771.

Woolhiser D.A., Smith R.E. and Giraldez J.-V. (1996) Effects of spatial variability of saturated hydraulic conductivity on Hortonian overland flow. *Water Resources Research*, **32**(3), 671–678.

Woolhiser D.A., Smith R.E. and Goodrich D.C. (1990) *KINEROS, A Kinematic Runoff and Erosion Model: Documentation and User Manual*, U.S. Department of Agriculture, Agricultural Research Service: ARS-77, p. 130.

Wu Y.-H., Yevjevich V. and Woolhiser D.A. (1978) *Effects of Surface Roughness and its Spatial Distribution on Runoff Hydrographs*, Colorado State University Hydrology Paper No. 96: Fort Collins, p. 47.